Reflection colour changes in cholesteric liquid crystals after the addition and photochemical isomerization of mesogenic azobenzenes tethered to sugar alcohols†

Haruhisa Akiyama,*[a] Asuka Tanaka,[b] Hideo Hiramatsu,[b] Jun'ichi Nagasawa[a] and Nobuyuki Tamaoki‡*[a]

Received 15th January 2009, Accepted 19th May 2009
First published as an Advance Article on the web 1st July 2009
DOI: 10.1039/b900890j

We controlled reflection colour of the glass-forming cholesteric liquid crystals over the whole visible region using the smectic liquid crystalline photochromic dopants on the basis of the different mechanism from the conventional helical twisting power change, which gave rise to full-colour recording and display materials at a lower additive concentration than that reported previously. We simply tethered multiple mesogenic azobenzene units to sugar alcohols to obtain effective dopants in which the intramolecular mesogenic moieties could adopt smectic-like alignments. The new dopants that featured linear sugar alcohol backbones exhibited increasingly stable smectic phases upon increasing the number of mesogenic groups in the molecule; a corresponding cyclic sugar alcohol derivative exhibited no such smectic phase. Addition of these smectic liquid crystalline dopants to the glass-forming cholesteric liquid crystalline material induced increasingly larger pitch shifts upon increasing the number of intramolecular mesogenic groups in the dopant. Dopants prepared from stereoisomeric sugar alcohol backbones provided similar liquid crystalline phases and induced similar pitch shifts after their addition to the cholesteric liquid crystals. The colour images recorded on the thin layer of the cholesteric liquid crystalline mixture were stabilized by fixing the cholesteric alignment into glassy states, which withstood heating at 70 °C.

1. Introduction

Cholesteric liquid crystals (ChLCs) find practical application in colour information technology.[1] The formation of the coloured state results from Bragg reflection of circularly polarized light from the periodically twisted structure in the ChLCs.[2] The biggest advantage of this method is the ability to realize rewritable colour displays because the cholesteric colour is tunable through reversible changes in the helical pitch of the twisted structure. It is known that the photochromic reactions of a small amount of photochromic compounds can reversibly control the properties of a large amount of the liquid crystals such as phase transitions and alignment directions.[3] Similarly, one well-established approach toward reversible control over the helical pitch employs photochemical reactions of photoresponsive additives doped into the ChLCs.[4–7] In general, the helical pitch shortens proportionally upon increasing the concentration of a chiral dopant when the ChLCs are composed of mixtures of nematic liquid crystals and small amounts of chiral compounds.[8] This means that the addition of a chiral dopant enforces a twisting of the cholesteric alignment. The proportionality constant in the relationship between the concentration and the helical pitch is referred to as the helical twisting power. Because this value depends on the relative content of the liquid crystal and dopant molecules, the change in chemical structure of a chiral photoresponsive dopant in response to light produces a change in its helical twisting power before and after irradiation, resulting in a change in the reflection colour of the ChLC. Another method to control the reflection colour is the addition of an achiral photoresponsive dopant into the ChLC.[4,6,7] Because the concentrations and chemical structure of the chiral compounds before and after irradiation are unchanged in this case, it is impossible to explain the phenomenon in terms of changes to the chiral twisting power. Indeed, the mechanism was not clear until recently. In 2003, we found that for achiral dopants added to glass-forming ChLCs, a relationship exists between the elongation of pitch and the increased contribution of cybotactic SmA clusters in the ChLC phase.[9] A cybotactic smectic cluster is a dynamic and fluctuating smectic-like domain observed in nematic phases.[10] The presence of cybotactic domains can be confirmed by the presence of layer structures in X-ray diffraction patterns. Such clusters are observed in the transition from nematic to smectic phases:[10] upon cooling from a nematic state, the contribution of the smectic cluster gradually increases with an increase in the cholesteric pitch prior to the transition to the smectic phase finally occurring. For this reason, the addition of

[a]*Nanotechnology Research Institute, National Institute of Advanced Industrial Science and Technology (AIST), Central 5, 1-1-1 Higashi, Tsukuba, Ibaraki, 305-8565, Japan. E-mail: h.akiyama@aist.go.jp; Fax: +81-298-61-4669; Tel: +81-298-61-4418*
[b]*College of Industrial Technology, Nihon University, 1-2-1 Izumi-cho, Narashino, Chiba, 275-8575, Japan*

† Electronic supplementary information (ESI) available: Characterization data; MALDI-TOF-MS and absorption spectra. See DOI: 10.1039/b900890j

‡ Present address: Research Institute for Electronic Science, Hokkaido University, N20, W10, Kita-ku, Sapporo, 001-0020, Japan. E-mail: tamaoki@es.hokudai.ac.jp; Fax: +81-11-706-9357; Tel: +81-11-706-9356.

a dopant that can stabilize the cybotactic smectic domain in a cholesteric phase should enlarge the cholesteric pitch. We have used glass-forming ChLCs having the dimesogenic structure **CD8** (Scheme 1) for full-colour recording. The LC alignment of **CD8** can be quickly rearranged at the cholesteric temperature (115–80 °C). Indeed, we can control the reflection colour in this LC temperature range within a few seconds and then fix the image by quickly cooling the sample into the glass state. Several kinds of photochromic additives for **CD8** have been used for photochemical tuning of the cholesteric colour.[5p,6,7] One of the most important requisites for these photochromic additives is for one of the isomers to have the ability to induce the cybotactic smectic domain in the host cholesteric liquid crystal, while the other isomer exhibits no such (or little) ability. Another requisite is that the glassy state of the mixture must exhibit thermal stability. Among the dopants tested, we found that achiral azobenzene oligomers with a side-chain liquid crystal structure possess superior properties relative to other additives in that they have both high thermal stability and the ability to induce a large pitch shift at low doping concentrations.[7] We deduced that the large pitch shift arose as a result of the molecular structure stabilizing the cybotactic smectic cluster of **CD8** because intramolecular mesogenic side chains of the oligomers can produce a layer-like (smectic-like) structure even in a molecularly dispersed state; they can stretch on both sides of main chain and align in a parallel manner. In fact, these dopants themselves exhibit an SmA phase with a layer structure in which the layer distance matches that of the cybotactic SmA of **CD8**. The other advantage of using oligomeric dopants is the good thermal stability of the colour images. Although addition of a low-molecular-weight compound to vitreous materials often decreases the glass transition temperature, **CD8** doped with the oligomeric dopants maintains its glassy state up to the same glass transition temperature as that of pure **CD8**. We have found, however, that although the oligomeric dopants possess good properties for use with ChLCs, sample preparation can be problematic for two reasons: (i) the oligomer is generally obtained in low yield because a chain transfer reagent, which decreases the synthetic yield, is used for the free radical polymerization to reduce the molecular weight of the polymer; (ii) strict and reproducible control over the molecular weight and dispersity are impossible in free radial polymerizations. Because the physical properties of low-molecular-weight polymers are strongly influenced by their molecular weight, the second problem is serious if oligomeric compounds are to be used widely. In this study, we synthesized new dopants featuring a single component molecule that can mimic the behaviour of azobenzene side chain oligomers. Sugar alcohols present multiple hydroxyl groups from a carbon chain backbone; their structures can be considered as an oligomer of hydroxymethylene units. In addition, because sugar alcohols are naturally derived, some of them are commercially available at low cost. To realize the bunch structure of multiple mesogenic side chains, we tethered azobenzene-based mesogenic moieties to several kinds of sugar alcohols. Sugar-based liquid crystalline materials prepared through substitution of some of the hydroxyl groups in the sugar

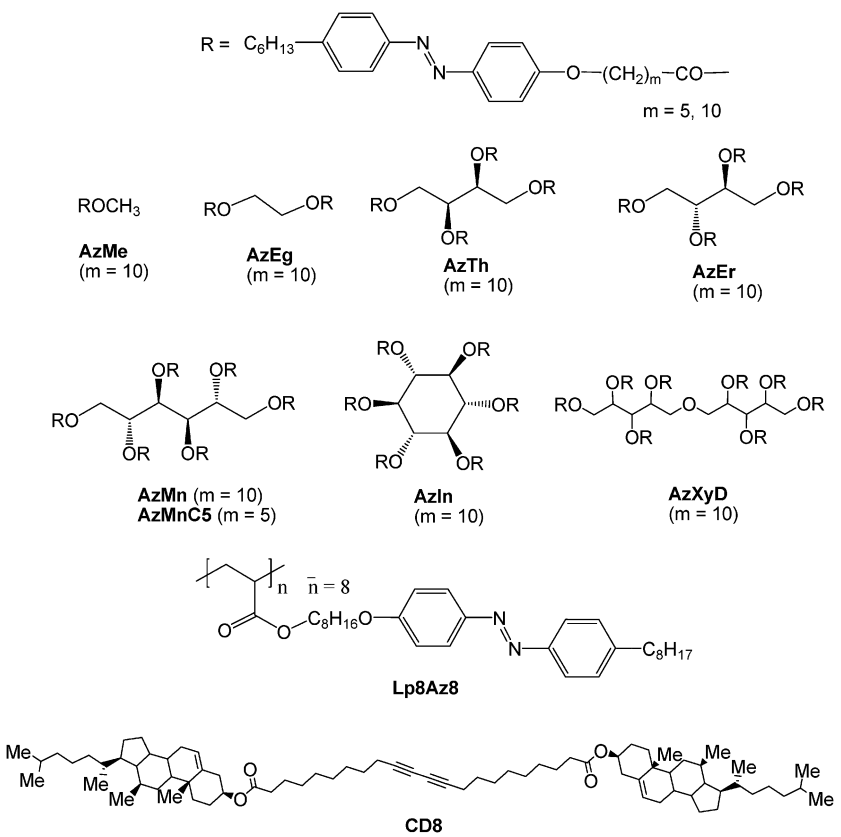

Scheme 1 Chemical structures of the mesogenic compounds, the sugar alcohol backbones, and the cholesteric liquid crystal.

with linear hydrophobic groups are well established; in these materials, the liquid crystallinity originates through phase separation of the hydrophobic and hydrophilic parts.[11] In this study, we used a sugar alcohol merely as a connector of multiple mesogens in the accurately controllable manner. We investigated the liquid crystalline properties of the resultant compounds and their properties as dopants for **CD8**. While several kinds of monodisperse main-chain liquid crystals[12] or liquid crystalline multipedes including dendritic molecules[13] have been reported, studies on monodisperse side-chain liquid crystalline oligomers with linear main chains are few. We systematically investigated the number effects of mesogenic side chains of the monodisperse side-chain liquid crystalline oligomers from a monomer to an octamer.

2. Results and discussion

2.1 Synthesis and liquid crystalline properties of azobenzene mesogens appended to sugar alcohols

To synthesize monomer, dimer, tetramer, hexamer, and octamer analogues, we used methanol, ethylene glycol, L-threitol, *meso*-erythritol, D-mannitol, *scyllo*-inositol, and xylitol dimer as backbones. We used the stereoisomers L-threitol and *meso*-erythritol, which possess four hydroxyl groups each, to investigate the effect of the stereochemical structure of the backbone on the cholesteric pitch. We employed D-mannitol and inositol, which contain six hydroxyl groups each, but linear and cyclic structures, respectively, to compare the effects of the topological structure of the dopant on the cholesteric pitch. Because sugar alcohols presenting eight hydroxyl groups are not commercially available, we synthesized the xylitol dimer as an analogue of an octamer using the method presented in Scheme 2. We performed esterification reactions of the acid chloride derivative R–Cl (m = 10) to functionalize the hydroxyl groups of the sugar alcohols with the mesogenic azobenzene units (Scheme 1). In addition, we synthesized another mannitol derivative through a reaction with the azobenzene acid chloride R–Cl (m = 5) to investigate the effect of the molecular chain length. Not all of the hydroxyl groups were esterified by the azobenzene derivatives at room temperature, indicating that severe steric hindrance existed around the hydroxyl groups of the sugar alcohols. Nevertheless, reactions performed at higher temperatures led to esterification of all of the hydroxyl groups with azobenzene moieties (see Experimental).

Table 1 lists the phase transition temperatures of these compounds, as estimated using dynamic scanning calorimetry (DSC) and polarizing optical microscopy (POM). The monomeric and dimeric azobenzene compounds, **AzMe** and **AzEg**, respectively, do not exhibit any mesophases. We observed

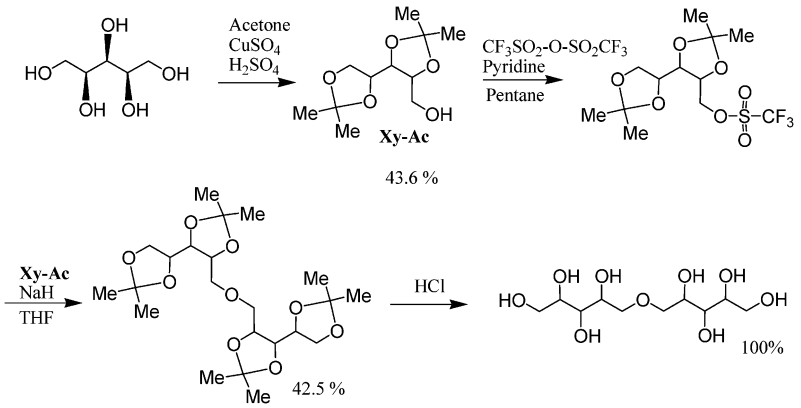

Scheme 2 Synthetic method for the preparation of the xylitol dimer.

Table 1 Physical characteristics of azobenzene compounds with alcohol backbones

	Alcohol	Cooling rate/°C min^{-1}	Transition temperature/°C	Layer distance /nm
AzMe	Methanol		Iso 65 Cr (Cr 72 Iso)	—
AzEg	Ethylene glycol	2	Iso 104 Cr	—
AzTh	L-Threitol	5	Iso 98 SmA 87 SmB 79 SmE	
		2	Iso 100 SmA 96 Cr	3.14 (SmB)
AzEr	*meso*-Erythritol	5	Iso 100 SmA 77 SmB 70 SmE	3.14 (SmA)
		2	Iso 101 SmA 89 Cr	3.13 (SmB)
AzMn	D-Mannitol	5	Iso 107 SmA 84 SmB	3.05 (SmA)
		2	Iso 109 SmA 86 SmB	3.11 (SmB)
AzIn[a]	*scyllo*-Inositol	2	Iso 162 Cr (Cr 171 Iso)	—
AzXyD	Xylitol dimer	2	Iso 113 SmA 85 SmB (SmB 87 SmA 114 Iso)	3.18 (SmA), 3.08 (SmB)
AzMnC5	D-Mannitol	2	Iso 118 SmA 59 SmB (SmB 61 SmA 121 Iso)	4.73 (SmA), 4.71 (SmB)

[a] Very small peaks were observed below melting points.

monotropic SmA, SmB, and SmE phases for the tetrasubstituted compounds **AzTh** and **AzEr**, but the corresponding peaks in their DSC curves were broad, partially overlapping, and changed shape depending on the cooling rate. When we maintained these samples at any temperature at which the materials exhibited SmA phases, we observed (POM) a transition to a higher-order smectic or crystal phase after 10–30 min. These gradual transitions at constant temperatures indicate that these SmA phases were thermodynamically unstable. These two tetrasubstituted compounds exhibited similar phase behaviour regardless of the configurations of their sugar backbones. Whereas one of our hexasubstituted compounds (**AzMnC5**) exhibited SmA and SmB phases on both heating and cooling, the other (**AzMn**) exhibited monotropic SmA and SmB phases only on cooling, but the two peaks corresponding to each transition were clearly separated and unaffected by the cooling rate. We observed thermodynamically stable (enantiotropic) SmA and SmB phases for the octasubstituted compound **AzXyD**. Taken together, the phase behaviour of these materials indicates a tendency for increased stabilization of the smectic phases upon increasing the number of azobenzene side chains. We suspect that the larger of these compounds can form structures similar to that of side chain-type liquid crystalline polymers, *i.e.*, parallel alignments of extended side chains on both sides of a backbone; such a parallel alignment can be stabilized through lateral interactions between pairs of mesogenic side chains and is enhanced upon increasing the number of side chains. The layer lengths of the smectic phases of the series of mesogenic compounds derived from R–Cl (m = 10) were 3.0–3.2 nm for both the SmA and SmB phases. In its fully extended trans conformation, the monomeric compound **AzMe** has a length of *ca.* 3.2 nm, which is almost equal to the smectic layer spacing. The smectic layer distance of 4.5 nm for **AzMnC5** does not match the molecular length (2.7 nm) of the model compound, R–OMe (m = 5), indicating the existence of an interdigitated layer structure. All of our compounds possessing four or more azobenzene moieties exhibited liquid crystalline phases, except for the hexasubstituted cyclic compound **AzIn**, which did not exhibit any mesophases. Because **AzIn** possesses six azobenzene units isotropically bonded to an inositol backbone in a two-dimensional surface, it is unlikely that a layer structure or a smectic phase would form. Thus, a linear backbone presenting several mesogenic side groups is necessary to produce the liquid crystalline material exhibiting smectic phases. Although **AzTh**, **AzMn**, and **AzMnC5** possess chiral backbones, we did not observe chiral mesophases originating from their molecular chirality.

2.2 Effect of additives on cholesteric pitch

We estimated the reflection band shifts of the glass-forming cholesteric liquid crystal **CD8** containing 2 wt% of each of our new compounds from the change in the reflection band position in the absorption spectra recorded after quenching the cholesteric alignment in these samples through rapid cooling from a liquid crystalline temperature (95 °C). Fig. 1 plots the differences in the reflection maximum wavelengths of **CD8** in the presence and absence of the additives; it reveals the abilities of the dopants to induce the cholesteric pitch shift. The addition of **AzTh**, **AzEr**, **AzMn**, or **AzXyD**, each of which individually

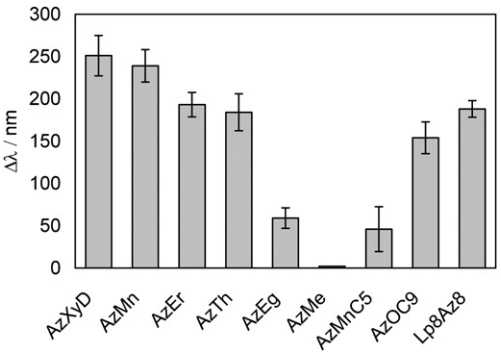

Fig. 1 Reflection colour shifts (Δλ/nm) of the films of **CD8** containing 2 wt% of the dopants, quenched from 95 °C. The values were estimated as averages from three–five measurements. Error bars represent standard deviations.

exhibits SmA phases, induced a large reflection colour shift. The values of the shifts observed after the addition of the tetrasubstituted compounds **AzTh** and **AzEr** were almost identical, but slightly smaller than those observed after the addition of **AzMn** and **AzXyD**. The addition of **AzEg** and **AzMe**, which individually exhibit no mesophases, induced small and very small shifts, respectively. The addition of **AzIn**, which also exhibits no mesophases, brought about no change in the reflection colour of **CD8**, presumably because of the immiscibility between **CD8** and **AzIn**, which we ascertained by observing a phase separated structure under POM. Taken together, these findings support our hypotheses that a large cholesteric pitch shift is induced after the addition of smectic compounds that have the potential to stabilize smectic clusters in the cholesteric phase. In terms of their stable smectic properties, we would predict that the pitch shift induced by **AzXyD**, with its greater number of side chains, should be superior to that of **AzMn**; in contrast, the pitch shifts induced by these two compounds were quite similar. To understand this behaviour, we should take into account the fact that **AzXyD** has a larger molecular weight than **AzMn** and, therefore, it was present at a lower molar concentration under conditions of a constant weight concentration. Therefore, we deduce that the negative effect that a lower concentration has on the pitch shift is balanced out by the positive effect of increasing the number of side chains, but only up to the hexamer level. The addition of **AzMnC5**, with its shorter alkyl chain length, induced much less of a colour change than did **AzMn**. A similar distinct dependence of the alkyl chain length has been observed previously for other dopants;[6a,7,9] it reflects the phenomenon that large pitch shifts can be induced only when the molecular length of the additive matches the layer distance of the smectic cluster in the ChLC. Indeed, the layer distances of the smectic phases of **AzTh**, **AzEr**, **AzMn**, and **AzXyD** (3.0–3.1 nm; see Table 1) as single components are very close to the layer length of the cybotactic smectic cluster in **CD8** (2.8 nm).[9] Therefore, we must select molecules of appropriate length for use as dopants. Our investigation of a series of monomeric compounds revealed, however, that not only is the molecular length important in causing a large pitch shift, but so too is the chemical structure. Among previously reported[6,7,9] monomeric dopants for **CD8**, we observed the largest pitch shift after the addition of 4,4′-bis(nonyloxy)azobenzene (**AzOC9**). The pitch shift was

smaller than those induced by **AzTh** and **AzEr**, but larger than that induced by **AzEg**. In contrast, the only monomeric analogue in our series of new compounds, **AzMe**, exhibited quite a small shift, suggesting that the structure of the mesogenic side chain moieties of our new dopants was not optimum. Conversely, it is a proof that the bundling of multiple mesogenic side chains is a useful method to obtain effective dopants—even for molecules featuring inappropriately designed mesogenic units. Fig. 2 shows X-ray diffraction (XRD) patterns for **CD8** containing 2 wt% of **AzMn** and **AzMe** at 95 °C, where the intensity is normalized at the maximum of the broad peaks around 17°. In both cases, the peaks corresponding to the layer distance of 2.8 nm are observed at 3.2°, and are considered to be derived from the cybotactic smectic A clusters. The peak of **CD8/AzMn** is higher and sharper than that of **CD8/AzMe**. For more detailed comparison, the intensity and sharpness (FWHM; full width at half maximum) of the XRD peaks of the several cholesteric mixtures are listed in Table 2. The **CD8** mixtures with **AzMn**, **AzEr**, **AzEg** and **AzMe**, which induced large pitch shifts in that order, exhibited the sharp and strong XRD peaks in the same order. The correspondence relation supports the hypothesis that enhancement of the cybotactic clusters upon addition of the dopants causes the cholesteric pitch shifts. Fig. 3 presents UV–Vis absorption spectra of the mixtures of **CD8** and each dopant in the forms of their cholesteric glassy films. The absorption peaks at *ca.* 350 nm and at longer wavelengths correspond to the π–π* transition of the *trans*-azobenzene moieties and to the reflection band, respectively. The expanded regions around the π–π* absorption band of the azobenzene moieties, presented in the inset to Fig. 3, reveals that the spectral shapes of the **CD8/AzMe** and **CD8/AzEg** systems were the same. The spectra of **CD8/AzMn** and **CD8/AzXyD** also had the same shapes, but they differed from those of **CD8/AzMe** and **CD8/AzEg** in that their absorption maxima appeared at shorter wavelength. The spectral shapes of **CD8/AzTh** and

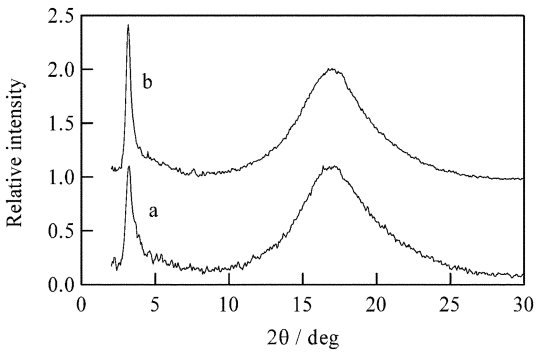

Fig. 2 X-Ray diffraction patterns for **CD8** containing 2 wt% of **AzMe** (a) and **AzMn** (b) at 95 °C.

Table 2 Half-width and relative intensity of small-angle X-ray diffraction peaks at 3.2°

	FWHM/deg	Relative Intensity
CD8/AzMe	5.3	1.00
CD8/AzEg	4.9	1.16
CD8/AzEr	4.4	1.23
CD8/AzMn	3.8	1.41

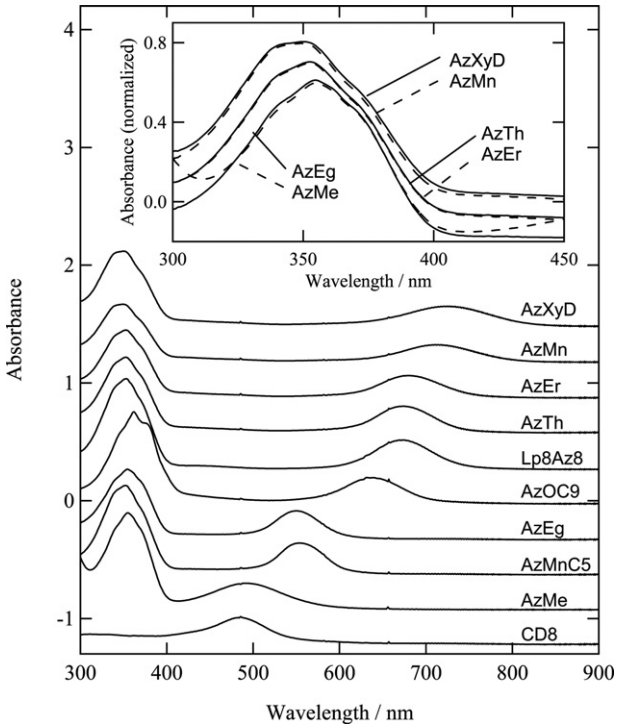

Fig. 3 UV–Vis absorption spectra of films of **CD8** containing 2 wt% of the dopants, quenched from 95 °C; inset: expanded region of selected spectra.

CD8/AzEr were also identical, with their signals positioned between those of the other two types of spectra. We conclude that three kinds of spectra existed, with the absorption maximum shifting to a shorter wavelength upon increasing the number of side chains. Because the position of the absorption maximum can reflect the conditions surrounding chromophores, these spectra suggest that the units in the dimer and monomer were surrounded by **CD8** molecules only; *i.e.*, the two azobenzene moieties of the dimer were extended to different directions. In the tetramers, hexamer, and octamer, the azobenzene side chains existed in a parallel alignment and were extended across both sides of the linear backbones, interacting with each other even in the molecularly dispersed media. This concept supports our hypothesis that such dopants have high abilities to stabilize smectic clusters and induce large pitch shifts. Therefore, fine-tuning the number of side chains is an important aspect of designing such systems. Indeed, these new compounds are the most effective dopants ever reported for **CD8**: the reflection colour shifts induced by **AzXyD** and **AzMn** are larger than those induced by the most effective oligomeric (**Lp8Az8**) and monomeric (**AzOC9**) compounds.[5p,6,7,9]

2.3 Photoinduced pitch shift and photoimaging

Azobenzene is famous as a photochromic compound that isomerizes reversibly from *E* to *Z* upon irradiation with UV light and from *Z* to *E* upon irradiation with visible light. Adding certain types of azobenzene derivatives as *E* isomers to **CD8** often induces a large pitch shift; photochromic reactions to the corresponding *Z* isomers lead the system to almost recover to its original state.[5p,6,7] We investigated the photoresponse of our new dopants in cholesteric mixtures. Fig. 4a displays the

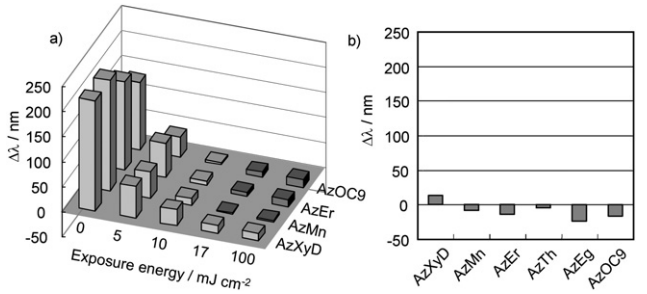

Fig. 4 a) Photochemical change in the reflection colour shifts (Δλ/nm) of **CD8** doped with 2 wt% of **AzXyD**, **AzMn**, **AzEr**, or **AzOC9** before and after UV irradiation (365 nm) at different energies; dark gray bars represent negative values. b) Reflection colour shifts of the new dopants and **AzOC9** upon irradiation with UV light at 100 mJ cm^{-2}.

photoinduced shifts of **CD8** doped with 2 wt% of **AzXyD**, **AzMn**, **AzEr**, and **AzOC9** before and after UV irradiation (365 nm). The reflection band shifted to shorter wavelength upon increasing the irradiation energy; it was accompanied by a decrease in the absorption at 360 nm arising from *E*–*Z* isomerization (ESI† Fig. S2). The photoinduced shifts in reflection colour were almost complete after irradiation at 17 mJ cm^{-2}, regardless of the nature of the dopant. Isomerization still proceeded when irradiated at light energies of up to 100 mJ cm^{-2}. Fig. 4b reveals that the reflection colour shifts induced by our new dopants and by **AzOC9** upon irradiation with UV light at 100 mJ cm^{-2} were all slightly negative, except for that induced by **AzXyD**, which was slightly positive. Nevertheless, in all cases these values were almost all equal to zero, which corresponded to a blue reflection colour. This phenomenon can been explained by considering that the *E* isomer of azobenzene can behave as a mesogenic core that affects the cholesteric pitch, whereas the bent structure of the *Z* isomer cannot exist as a mesogenic core that interacts with host LC molecules. For full-colour recording, the wavelength of the reflection band should exist in the infrared region (>700 nm) prior to irradiation to ensure a colourless state. If this condition is satisfied, irradiation for a shorter period of time can also give rise to green or red reflections. Therefore, we expected that we could control the cholesteric colour through photochemical reactions using some of our new dopants that induce large pitch shifts. To realize a colourless state for full-colour recording, we adopted a cholesteric mixture including 3 wt% of each dopant. We recorded colour images in a 1.8 × 1.8 cm cell using a maskless irradiation device that generated UV light of different intensity for each 1024 × 764 pixel. After fixing the recorded images in the glassy LC through rapid cooling, we heated the films to estimate the thermal stability of their images. Fig. 5 displays photographs of images recorded in films obtained from a mixture of **CD8** and **AzMn** before and after heating for 30 min at various temperatures. The colour image that formed in the cholesteric glassy film remained unchanged when heating at temperatures up to 70 °C. We observed similar thermal stabilities for the images recorded in mixtures of **CD8** and **AzTh**, **AzEr**, and **AzXyD**; these stabilities are comparable to those observed for mixtures of **CD8** and oligomeric dopants. The thermal stability of the mixture of **CD8** and **AzEg** was low (upper limit: 40 °C), which can be explained by considering the severe impurity effect of the low-molecular-weight dopant, which lowered the glass transition temperature of the matrix.

Fig. 5 Colour pictures, prepared using the maskless irradiation system, recorded in a thin film of **CD8** doped with 3 wt% of **AzMn**. (a) Before heating; (b, c) after heating for 30 min at b) 70, and c) 80 °C.

3. Conclusion

Although oligomeric mixtures of achiral dopants are effective at controlling the cholesteric reflection colour, in this study we synthesized single-component analogues of these oligomers. Fig. 6 provides schematic representations of these new dopants and summarizes the results we obtained. Because we controlled the number of intramolecular mesogenic side chains, we could determine the optimal number required to induce the largest pitch shift. In addition, because we prepared isomers presenting the same number of mesogenic side chains, we could elucidate the effects of the configuration and topological structure (linear or cyclic) of the main chains. We found that using a linear backbone was necessary to induce a large pitch shift, but differences in the configuration of the main chain had little effect. The dopants possessing linear backbones exhibited stable smectic phases that increased in stability upon increasing the number of side chains; the ability to induce a pitch shift increased accordingly. These results support our recently proposed mechanism: that the enlarged cholesteric pitch induced by an achiral dopant originates from the stabilizing effect of the dopant on the cybotactic smectic cluster in the cholesteric phase. Using our newly synthesized dopants, we recorded full-colour images that exhibited high thermal stability.

4. Experimental

4.1 Materials

The preparation of **CD8** has been reported previously.[14] Azobenzene alkyl acids were synthesized using a method similar to that described in the literature.[15]

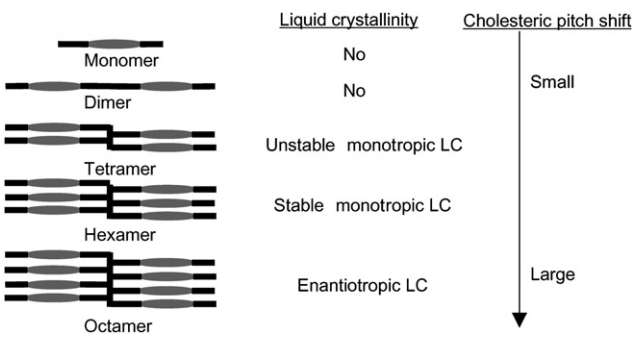

Fig. 6 Schematic representations of the new dopants and a summary of the results.

2,3:4,5:2′,3′:4′,5′-Tetra-*O*-isopropylidene-1,1′-oxybis(1-deoxyxylitol). 1,2:3,4-Di-*O*-isopropylidenexylitol[16] (1.27 g) and sodium hydride (65% suspension in oil, 0.4 g) were dissolved in dry tetrahydrofuran (THF, 50 mL) at room temperature and then a solution of 1:2,3:4-di-*O*-isopropylidene-5-*O*-trifluoromethanesulfonylxylitol[17] (1.2 eq) in dry THF (25 mL) was added slowly. The mixture was stirred for 12 h at room temperature. The solution was diluted with EtOAc and washed with brine. After evaporating the solvent, the crude compound was purified through column chromatography (SiO_2; CH_2Cl_2/EtOAc, 4:1) to yield a transparent liquid (1.04 g, 42.5%). ^{1}H NMR ($CDCl_3$, δ): 1.39 (s, 6H, CH_3), 1.43 (s, 18H, CH_3), 3.64–3.70 (m, 4H, CH_2O), 3.81–3.93 (m, 4H, CH_2), 4.00–4.22 (m, 6H, CH). MALDI-TOF-MS: *m*/*z* calcd. for $[M + Na]^+$ and $[M + K]^+$, 469.24 and 485.21 respectively; found 469.61, 485.58 respectively.

1,1′-Oxybis(1-deoxyxylitol). 1:2,3:4-Di-*O*-isopropylidene-5-*O*-trifluoromethanesulfonylxylitol (1.04 g) was suspended in 2 M HCl (50 mL) and then MeOH was added to form a homogenous solution. The mixture was stirred at 90 °C for 6 h and then the solvent was evaporated under vacuum to yield a sticky liquid (0.67 g). ^{1}H NMR (CD_3OD, δ): 3.53–3.70 (m, 10H, CH, CH_2), 3.73–3.79 (m, 2H, CH), 3.85–3.93 (m, 2H, CH_2). ESI-TOF-MS: calcd. for $[M + Na]^+$ *m*/*z* 309.12; found 309.1.

Esterification. The reaction procedure for the synthesis of **AzXyD** is described below as a typical example. The other compounds were synthesized in a similar manner. The purification methods, synthetic yields and physical data of other compounds, **AzMe**, **AzEg**, **AzEr**, **AzTh**, **AzMn**, **AzMnC5** and **AzIn**, are in the ESI.†

AzXyD. Thionyl chloride (1.2 mL) was added to a solution of 11-[4-(4-hexylphenylazo)phenoxy]undecanoic acid (1.00 g, 2.14 mmol) in dry CH_2Cl_2 (3.5 mL). After stirring the solution for 1 h, the solvents were evaporated under vacuum. The red residue was dissolved in CH_2Cl_2 (6 mL) and then this solution was added dropwise to a solution of the xylitol dimer (0.051 g, 0.17 mmol) in pyridine (4 mL). After heating under reflux for 24 h under a dry nitrogen atmosphere, the solution was diluted with CH_2Cl_2 and washed several times with water. The organic phase was dried ($MgSO_4$) and then the solvent was evaporated. The residue was dissolved in a small amount of CH_2Cl_2, placed in a flask and sealed with a plug. The flask was heated at 60 °C for 12 h to ensure complete thermal isomerization of all the azobenzene units to their *E* isomers. After evaporating the solvent, the residue was purified twice by column chromatography through SiO_2, eluting once with CH_2Cl_2/hexane (2:1) and then with CH_2Cl_2 alone under red light. The hepta, hexa, and lower-order substituted compounds generated as byproducts were thoroughly removed. The product was obtained as an orange solid (0.2 g, 30%). ^{1}H NMR ($CDCl_3$, δ): 0.88 (t, $J = 6.3$ Hz, 24H, CH_3), 1.30 (s, 124H, CH_2), 1.44 (br s, 16H, $CH_2C_2H_4OAr$), 1.61 (m, 32H, CH_2CH_2Ar, CH_2CH_2COO), 1.78 (q, $J = 7.0$ Hz, 16H, CH_2CH_2OAr), 2.31 (br s, 17H, CH_2COO), 2.65 (t, $J = 7.6$ Hz,16H, CH_2Ar), 3.40–3.60 (m, 4H, H-1a, H-1b, H-1′a, H-1′b), 3.99 (t, $J = 6.2$ Hz, 18H, OCH_2, H-5a, H-5′a), 4.28–4.40 (m, 2H, H-5b, H-5′b), 5.10–5.20 (m, 2H, H-2, H-2′), 5.25–5.36 (m, 2H, H-4), 5.38–5.50 (m, 2H, H-3), 6.94 (d, $J = 8.8$ Hz, 16H, ArH), 7.29 (d, $J = 8.6$ Hz, 16H, ArH), 7.78 (d, $J = 8.2$ Hz, 16H, ArH), 7.87 (d, $J = 8.8$ Hz, 16H, ArH). MALDI-TOF-MS: calcd. for $[M + Na]^+$ and $[M + K]^+$, 3897.6 and 3913.6, respectively; found 3896.8 and 3913.7, respectively. Elemental analysis. Found: C, 75.20; H, 8.81; N, 5.73. Calcd. for $C_{240}H_{338}N_{16}O_{25}$: C, 74.92; H, 8.86; N, 5.82%.

4.2 LC cell preparation

CD8 was mixed at 125 °C with 2 or 3 wt% of the dopant and 5 μm diameter epoxy resin spheres (<0.1 wt%; Nippon Shokubai). The molten mixture was placed between two glass slides on a hot stage (Mettler FP(82) heated at 125 °C. The isotropic phase transformed into the LC phase upon cooling to 95 °C; the sample was then dropped into iced water. This rapid cooling technique froze the LC alignment into the glassy state.

4.3 Physical measurements

Matrix-assisted laser desorption ionization time-of-flight mass spectrometry (MALDI-TOF MS) was conducted using an Applied Biosystems Voyager-DE Pro instrument operated in reflector mode; samples were prepared through mixing MeOH and CH_2Cl_2 solutions of the compounds with α-cyano-4-hydroxycinnamic acid. Electrospray ionization time-of-flight mass spectrometry (ESI-TOF MS) was conducted using an Applied Biosystems Mariner instrument. ^{1}H NMR spectra of samples dissolved in $CDCl_3$ were recorded using a Varian Gemini-300 BB spectrometer. Absorption spectra were measured using a Hewlett–Packard UV–Vis spectrophotometer (Agilent 84(53). DSC measurements were conducted using a Seiko DSC Exstar 6000 instrument operated at heating rates of 5 and 2 °C/min. Photoimaging and UV irradiation were performed using a maskless UV exposure instrument (Interwave) and a modified DLP projector system that generated pixelated 365 nm light (1024 × 764 dots). The intensity of the light at each dot was modulated using a digital micromirror device; the image data were provided by a JPEG file from a personal computer. Small-angle X-ray diffractometry was conducted as reported earlier;[7] the X-ray exposure time was 15 min.

References

1 N. Tamaoki, *Adv. Mater.*, 2001, **13**, 1135, and references cited therein.
2 (*a*) P. G. de Gennes, J. Prost, *The Physics of Liquid Crystals*, Clarendon Press, Oxford, UK, 1993, Section 6.1. p 219; (*b*) D. Demus, J. Goodby, G. W. Gray, H.-W. Spiess, V. Vill, *Handbook of Liquid Crystals, Vol. 2A*, Wiley-VCH, Weinheim, 1998, (Ch. IV 2.2.1), p 335.
3 (*a*) K. Ichimura, *Chem. Rev.*, 2000, **100**, 1847, and references cited therein; (*b*) T. Ikeda, *J. Mater. Chem.*, 2003, **13**, 2037, and references cited therein; (*c*) C. K. Prasad, G. G. Nair and G. Hegde, *Adv. Mater.*, 2005, **17**, 2086.
4 (*a*) E. Sackmann, *J. Am. Chem. Soc.*, 1971, **93**, 7088; (*b*) S. Z. Janicki and G. B. Schuster, *J. Am. Chem. Soc.*, 1995, **117**, 8524.
5 (*a*) B. L. Feringa, N. P. M. Huck and H. A. van Dorenl, *J. Am. Chem. Soc.*, 1995, **117**, 9929; (*b*) R. A. van Delden, M. B. van Gelder, N. P. M. Huck and B. L. Feringa, *Adv. Funct. Mater.*, 2003, **13**, 319; (*c*) A. Yu. Bobrovsky, N. I. Boiko and V. P. Shibaev, *Adv. Mater.*, 1999, **11**, 1025; (*d*) P. van de Witte, E. E. Neuteboom, M. Brehmer and J. Lub, *J. Appl. Phys*, 1999, **85**, 7517; (*e*) T. Sagisaka and Y. Yokoyama, *Bull. Chem. Soc. Jpn.*, 2000, **73**, 191; (*f*) H.-K. Lee, K. Doi, H. Harada, O. Tsutsumi, A. Kanazawa,

T. Shiono and T. Ikeda, *J. Phys. Chem.*, 2000, **104**, 7023; (*g*) C. Ruslim and K. Ichimura, *Adv. Mater.*, 2001, **13**, 37; (*h*) J. Lub, W. P. M. Nijssen, R. T. Wegh, J. P. A. Vogel and A. Ferrer, *Adv. Funct. Mater.*, 2005, **15**, 1961; (*i*) T. Yoshioka, T. Ogata, T. Nonaka, M. Moritsugu, S.-N. Kim and S. Kurihara, *Adv. Mater.*, 2005, **17**, 1226; (*j*) T. Mitsuoka, H. Sato, J. Yoshida, A. Yamagishi and Y. Einaga, *Chem. Mater.*, 2006, **18**, 3442; (*k*) U. A. Hrozhyk, S. V. Serak, N. V. Tabiryan and T. J. Bunning, *Adv. Mater.*, 2007, **19**, 3244; (*l*) Q. Li, L. Green, N. Venkataraman, I. Shiyanovskaya, A. Khan, A. Urbas and J. W. Doane, *J. Am. Chem. Soc.*, 2007, **129**, 12908; (*m*) M. Mathews and N. Tamaoki, *J. Am. Chem. Soc.*, 2008, **130**, 11409; (*n*) S. Pieraccini, S. Masiero, G. P. Spada and G. Gottarelli, *Chem. Commun.*, 2003, 598–599; (*o*) S. Pieraccini, G. Gottarelli, R. Labruto, S. Masiero, O. Pandoli and G. P. Spada, *Chem. Eur. J.*, 2004, **10**, 5632; (*p*) N. Tamaoki, Y. Aoki, M. Moriyama and M. Kidowaki, *Chem. Mater.*, 2003, **15**, 719.

6 (*a*) N. Tamaoki, S. Song, M. Moriyama and H. Matsuda, *Adv. Mater.*, 2000, **12**, 94; (*b*) M. Moriyama, S. Song, H. Matsuda and N. Tamaoki, *J. Mater. Chem.*, 2001, **11**, 1003; (*c*) R. Davis, V. A. Mallia, S. Das and N. Tamaoki, *Adv. Funct. Mater.*, 2004, **14**, 743.

7 H. Akiyama, V. A. Mallia and N. Tamaoki, *Adv. Funct. Mater.*, 2006, **16**, 477.

8 P. G. de Gennes, J. Prost, *The Physics of Liquid Crystals*, Clarendon Press, Oxford, UK, 1993, Section 6.2. p. 239.

9 M. Kidowaki, M. Moriyama, M. Wada and N. Tamaoki, *J. Phys. Chem. B*, 2003, **107**, 12054.

10 D. Demus, J. Goodby, G. W. Gray, H.-W. Spiess, V. Vill, *Handbook of Liquid Crystals, Vol. 1*, Wiley-VCH, Weinheim, 1998, (Ch. VII 6.3.2), p. 380; Ch. VIII 3.6.2, p. 650.

11 (*a*) G. A. Jefferey and L. M. Wingert, *Liq. Cryst.*, 1992, **12**, 179, and references cited therein; (*b*) H. A. van Doren, E. Smits, J. M. Pestman, J. B. F. N. Engberts and R. M. Kellogg, *Chem. Soc. Rev.*, 2000, **29**, 183, and references cited therein; (*c*) S. Das, N. Gopinathan, S. Abraham, N. Jayaraman and M. K. Singh, *Adv. Funct. Mater.*, 2008, **18**, 1632.

12 (*a*) C. T. Imrie and P. A. Henderson, *Curr. Opin. Colloid Interface Sci.*, 2002, **7**, 298, and references cited therein; (*b*) I. Nishiyama, J. Yamamoto, J. W. Goodby and H. Yokoyama, *J. Mater. Chem.*, 2003, **13**, 2429; (*c*) C. V. Yelamaggad, I. S. Shashikala and Q. Li, *Chem. Mater.*, 2007, **19**, 6561.

13 (*a*) I. M. Saez and J. W. Goodby, *J. Mater. Chem.*, 2005, **15**, 26, and references cited therein; (*b*) Y. Shimizu, A. Kurobe, H. Monobe, N. Terasawa, K. Kiyohara and K. Uchida, *Chem. Commun.*, 2003, 1676.

14 N. Tamaoki, A. V. Parfenov, A. Masaki and H. Matsuda, *Adv. Mater.*, 1997, **9**, 1102.

15 T. Seki, T. Fukuchi and K. Ichimura, *Bull. Chem. Soc. Jpn.*, 1998, **71**, 2807.

16 R. M. Hann, A. T. Ness and C. S. Hudson, *J. Am. Chem. Soc.*, 1944, **66**, 73.

17 S. Solyon, K. Szilagyi and L. Toldy, *Liebigs Ann. Chem.*, 1987, 153.